

## Atomic Imaging of Particle Surfaces

L. D. Marks<sup>1,3</sup> and David J. Smith<sup>2,4</sup>

<sup>1</sup>Department of Physics, Arizona State University, Tempe, AZ 85287

<sup>2</sup>High Resolution Electron Microscope, Department of Metallurgy, University of Cambridge, Cambridge CB2 3RQ, England

High resolution electron microscopy has recently demonstrated the capability to directly resolve the atomic structure of surfaces on small particles and thin films. In this paper we briefly review experimental observations for gold (110) and (111) surfaces, and analyse how these results when combined with theoretical and experimental morphological studies, influence the interpretation of geometrical catalytic effects and the transfer of bulk surface experimental data to heterogeneous catalysts.

During the last twenty years, small metal particle systems, often model catalysts or commercial heterogeneous catalysts, have been extensively studied by electron microscopy. The primary objective has been to characterise their chemical and structural nature, with the intention of eventually understanding the nucleation and growth of small clusters as well as heterogeneous catalysis. In the process, essentially the whole range of electron microscope imaging techniques have been used. Conventional bright field and dark field techniques are illustrated by the classic work of Ino (1), and Ino and Ogawa (2). More sophisticated dark field techniques have also been developed which give improved particle contrast, such as selected zone dark field (3), annular dark field (4), and weak beam dark field (5). Other approaches, primarily using a scanning transmission instrument, have also been developed which produce analytical information (e.g. 6-8). Some recent reviews of these techniques can be found elsewhere (9-12) and reference should be made to the article by J.M. Cowley in these proceedings.

All of these methods suffer from one serious shortcoming - the spatial resolution is relatively poor ( $\sim 10\text{\AA}$ ) and information about the catalytically interesting region of the particle, namely the surface structure, is then not available. One particular technique, high resolution electron microscopy, has for many years been slowly

<sup>3</sup>Current address: Department of Materials Science and Ipatieff Laboratory, Northwestern University, Evanston, IL 60201

<sup>4</sup>Current address: Center for Solid State Science, Arizona State University, Tempe, AZ 85287

0097-6156/85/0288-0341\$06.00/0  
© 1985 American Chemical Society

progressing towards this goal. Although useful results were obtained using the technique to unravel complicated particle structures (13-17), surface information remained unavailable except for a few unusually favorable circumstances (e.g. 18).

As a result of technical improvements (19) to the Cambridge High Resolution Electron Microscope (20), we have recently succeeded in directly resolving the atomic structure of surfaces on small particles and thin films (21-27). This has included the first direct observation of a surface reconstruction, the so-called missing row model (28) of the 2x1 (110) gold surface (see Figure 1 and 21,22), effects due to elastic and plastic deformations at surfaces (see Figures 2 and 3 and 23,26) and details of surface steps and faceting (see Figures 4,6 and 21,27). In this paper we briefly describe the principle of the technique, review these observations, and consider their implications with respect to geometrical effects, linking the experimental data with theoretical analyses.

### Basis of the Technique

The technique employs a beam of swift (~500kV) electrons grazing the surface of interest. Provided that the beam is accurately aligned along a crystal zone axis, and that the electron-optical imaging system is adequate, then images are obtained which appear to show the atomic surface structure in profile (see Figure 1).

Interpretation of these images is both complicated and simple. With any electron microscope technique, the final image is the result of a complicated diffraction and lens aberration process and it is necessary to avoid the trap of naive interpretation, that seeing is believing. It is generally accepted that detailed calculations are required to confirm image interpretations, particularly for high resolution imaging, but also for other techniques. Fortunately, in most cases, high resolution images are faithful representations of the surface structure. The reasons for this are discussed in detail in 25,29,30, and can be summarised thus. With swift electrons and a heavy element, the electron waves channel (e.g. 30-32) down the atomic columns (for a crystal zone-axis orientation) with minimal cross-talk between adjacent columns. With optimal imaging conditions, primarily depending on the objective lens defocus, the spherical aberration and the damping effects of the microscope instabilities balance each other out (25,29). The final image is then an accurate local representation of the object, and it is correct to believe what is seen. Monolayer sensitivity and, with some care, limited sensitivity to chemical impurities can be achieved (25). When these conditions are not met an averaged (over the object) image is obtained rather than a local one and measurement of, for instance, surface relaxations is well nigh impossible.

### Results

Gold (110). The gold (110) surface has been observed to undergo a 2x1 reconstruction, with every other surface column missing, as shown in Figure 1. This particular image is from a particle of approximately 300Å in radius, and elements of the reconstruction were also observed on smaller particles (~100Å in radius). One interesting feature of the reconstruction is a 20 ± 5% expansion at the top of

the corrugated structure which becomes apparent in careful, digital comparisons of experimental and calculated images (22). This expansion has recently been confirmed by X-ray grazing incidence diffraction and ion scattering experiments (33,34).

Gold (111). The main feature of the gold (111) surface is that the surface mesh expands relative to the bulk - there is a tangential surface pressure (23,26,35). This behaviour manifested itself during an electron beam induced etching of contaminant carbon layers (by water vapour) as a "hill and valley" reconstruction, as shown in Figure 2. This is a roughening mechanism which provides space for an expansion to occur which is eventually accommodated by surface dislocations, essentially misfit dislocations to accommodate the surface pressure (see Figure 3). It is important to recognise here that the nature of the specimen used for electron microscopy differs from the bulk surfaces studied by, for instance, LEED. With a bulk surface we might expect some manifestation of the surface expansion other than a hill and valley roughening.

It is interesting to consider this surface as if it were an epitaxial system, that is a monolayer of gold epitaxed on a gold (111) surface. With any epitaxial system, provided that the misfit between the adsorbate and the substrate is small, the adatoms are elastically strained to the substrate surface mesh yielding pseudomorphic growth (for a review see, for instance, 36). For an infinite surface the strain is purely homogeneous, but with a finite adsorbed layer there is some buckling due to the implicit boundary condition of no tractions at the edges of the layer (37,38). This buckling also appears in some of the earlier analyses of surfaces using simple Morse potentials (e.g. 39) since these have an inbuilt expansive surface pressure. If the misfit between the adsorbate and the substrate is sufficiently large, it becomes energetically favorable to nucleate misfit dislocations to relieve the strains. Numerical calculations by Snyman and Snyman (40) for the case of a (111) layer on a (111) substrate show that Shockley partial dislocations and stacking faults are a low energy mechanism for this strain relief, correlating with the case of silver epitaxed on gold (111) (40). These calculations are in excellent agreement with our results.

Benzene on Gold (111). One chemically interesting event seen on the gold (111) surface was the formation of a benzene monolayer during the etching of the initial carbon contaminant layer by water vapour (25,26). This is a flat  $\pi$ -bonded layer, with a benzene to benzene spacing of 7.3 (+0.2)Å, and is shown in Figure 4. It is interesting to connect this observation with the mechanism of the etching process, which is probably similar to that of the water-gas reaction. We would hypothesise that the carbon acts as a temporary sink for the hydrogen during the etching with the initial reaction products being hydrocarbons and carbon monoxide. With various cracking reactions taking place under the electron beam, benzene can be one of many reaction products. Since benzene is probably relatively radiation resistant, particularly when  $\pi$ -bonded to a metal which can act as an energy sink, it could be a favored metastable product. There could also be some catalytic effect from the gold substrate.

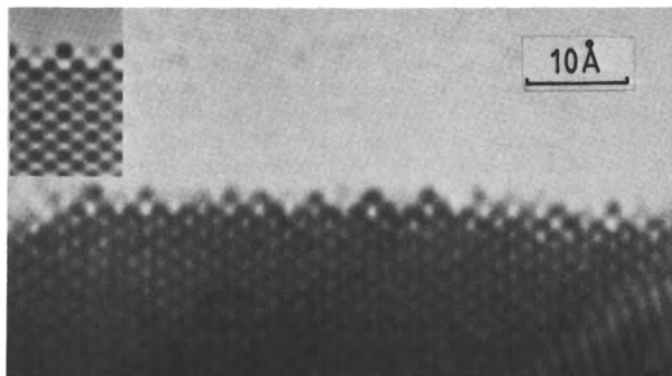


Figure 1. Area of rough gold (110) 2x1 reconstruction, with a numerical calculation inset - see 22. Atomic columns are black.

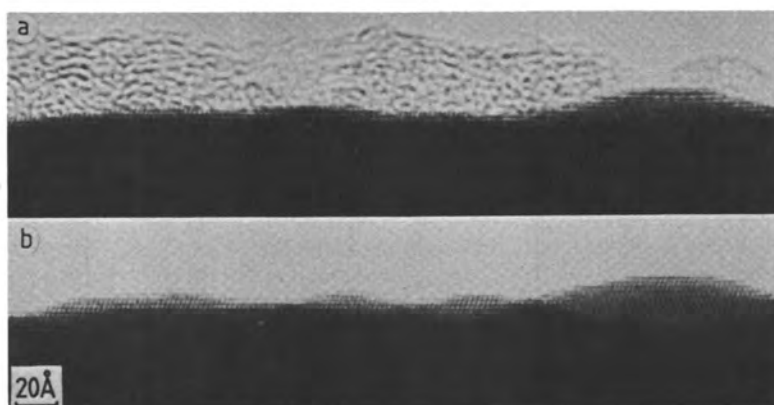


Figure 2. Hill and valley roughening of a gold (111) surface in a) before roughening (carbon covered) and b) following carbon removal.

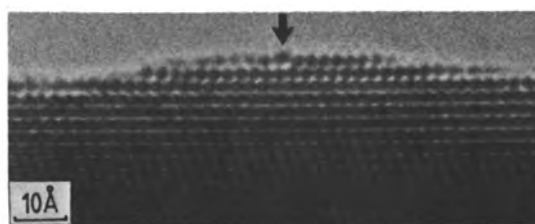


Figure 3. Area of clean gold (111) surface showing a surface Shockley partial dislocation (arrowed) - see 26. Atomic columns are black.

### Geometric Effects

There are a number of concepts concerning the structure of small particles which have a bearing upon geometrical catalytic effects (e.g. 41-43). These follow both from the surface imaging results, and a detailed experimental (13-15) and theoretical (44-47) study of particle morphologies.

Finite size effects. It is well known that, as the size of an atomic cluster drops, the relative proportion of edge and surface atoms increases. However, calculations of the relative fraction of these different surface sites have to date made one important assumption, namely that the external morphology of the particle remains constant. This assumption is not in fact valid; edge atoms for example have a higher intrinsic energy than surface atoms, so it is possible that a morphological change could occur which would minimise the number of edge atoms.

Detailed calculations (47) show that effects from the edge atoms are present and that there is also a stronger effect which can be linked to sphere packing. The number of atoms on a particular face, or in the cluster, deviates substantially from the continuum value (parameterised in terms of the surface area and cluster volume respectively) when the particles are small. This introduces further large edge-like terms in the total particle energy which will drive substantial morphological changes. For instance, for a simple broken bond model of an fcc particle restricted to having only (111) and (100) faces, the fraction of (100) surface drops markedly as the cluster size decreases as shown in Figure 5. This effect only occurs when the cluster energy is minimised with respect to its morphology.

It is also possible to have discrete microfacetting in small particles. For a large (essentially continuum) crystal, vicinal surfaces are important, their role being well understood through the Wulff construction (e.g. 48-50). However, the unit cell of a vicinal surface is large, and there may be insufficient space on a small particle. Only small unit mesh surfaces can be accommodated, and this can lead to microfacetting, a possible example being shown in Figure 6. We note that there is a likely catalytic particle size effect here in the disappearance of vicinal surfaces.

Boundary Conditions. The implicit boundary condition of small surface area can affect surface reconstructions and chemisorption. Surface steps, for example, are important for reconstructions (e.g. 51), and can determine the particular domain that occurs (e.g. 52). An example of a structural effect is on the gold (111) surface where there is an in-plane tangential surface pressure (23,26,35). On extended surfaces, a hill-and-valley roughening occurs to accommodate the expansion, as described earlier. In contrast, small particles accommodate the pressure by a surface buckle (26). We would expect similar behaviour when there is chemisorption involving interactions between the adsorbed molecules.

Gas-Particle effects. The gas environment and chemical impurities, such as promoters or poisons, can strongly influence the total particle morphology (49,50,53,54). Effects can occur via morphological changes which may eliminate or promote certain

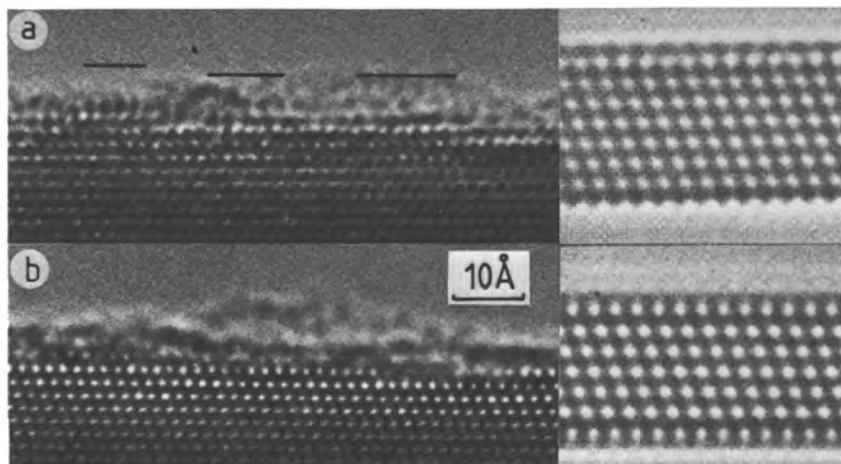


Figure 4. Area of benzene covered gold (111) surface, for two different objective lens defoci as required for unique image interpretation (see 24, 25). In a) the gold atomic columns are black, in b) white. Moiré fringes, rather than any true structural image, result from the benzene monolayer. Simulations (right) have benzene overlay on top surface only.

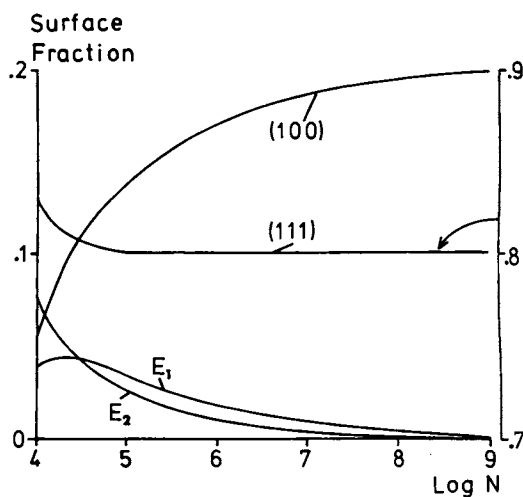


Figure 5. Relative fraction of the different surface atoms as a function of  $\text{Log } N$ , where  $N$  is the number of atoms, for a (111) and (100) faceted f.c.c. crystal when the surface morphology is equilibrated.  $E_1$  refers to the edges between the (100) and (111) faces,  $E_2$  to the edges between two (111) faces. The (111) curve is drawn using the axes to the right.

(catalytically important) facets. (For a review of effects on large surfaces see 12,49 and 50). This is equivalent to the blocking of an enzyme via a conformational change, rather than a direct attack upon the active site.

One example of this type of process arises in gold particles. When grown in UHV, the stable structures are in the form of non-crystallographic particles called multiply twinned particles or MTPs (1,2,13,15,44-46,55 and see Figure 7). In-situ experiments by Yagi et al (56), who observed the formation of MTPs both during growth and following coalescence, demonstrated that these particles are thermodynamically preferred when small (see also 44). However, specimen catalysts produced by Avery and Sanders (56) did not show significant concentrations of MTPs, which would appear to contradict the stability results of Yagi et al (56).

The difference can probably be attributed to the effects of trace water vapour, which experimentally inhibits gold MTP formation (26 and Figure 8), and which we suspect was present during the preparation of Avery and Sanders. The theoretical explanation is through the change in surface free energy and tangential surface pressure with contaminants, since both affect the energy balance between MTPs and single crystals (46). The surface pressure term is probably dominant, with the surface expansion upon the clean gold

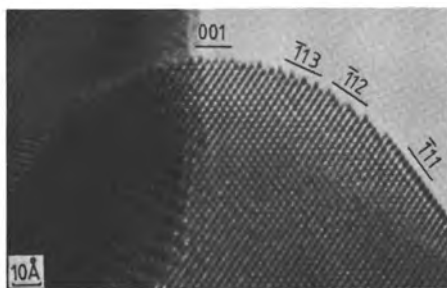


Figure 6. Microfaceted region of a gold crystal, with the facet indexing marked. The atomic columns are black.

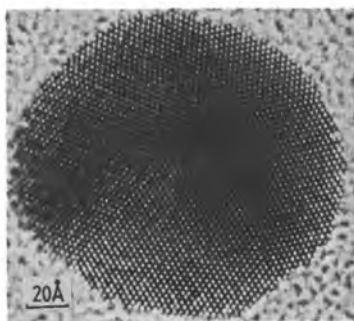


Figure 7. A decahedral MTP of gold showing white atomic columns, supported on an amorphous carbon film - see 15. An explanation of the complicated faceting of MTPs is given in 45.

American Chemical Society  
Library

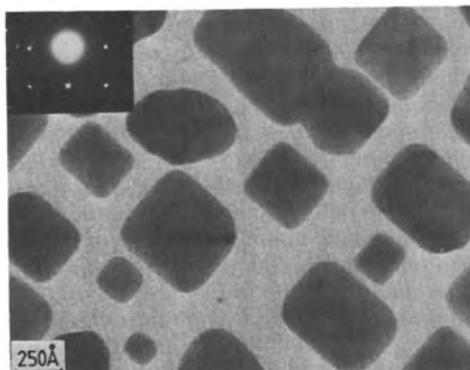


Figure 8. Image and diffraction pattern from an (100) epitaxial specimen of gold prepared in an unbaked UHV evaporator by deposition onto KCl and then transfer onto amorphous carbon. Here water vapour was the dominant residual gas (determined by mass spectrometry). The particles are square pyramidal single crystals.

(111) surface (23,26) presumably being suppressed by water adsorption, thus favoring single crystal formation. There are good theoretical reasons (35) for believing that similar effects can occur in other systems.

### Conclusions

We have discussed here, very briefly, some recent observations of small particle surfaces and how these relate to geometrical catalytic effects. These demonstrate the general conclusion that high resolution imaging can provide a direct, structural link between bulk LEED analysis and small particle surfaces. Apart from applications to conventional surface science, where the sensitivity of the technique to surface inhomogeneities has already yielded results, there should be many useful applications in catalysis. A useful approach would be to combine the experimental data with surface thermodynamic and morphological analyses as we have attempted herein. There seems no fundamental reason why results comparable to those described cannot be obtained from commercial catalyst systems.

### Acknowledgments

The authors would like to thank Drs. A. Howie, V. Heine, E. Yoffe, R.F. Willis, J.M. Cowley and J.A. Venables for advice and comments during the course of this work. We acknowledge financial support from the SERC, U.K. and L.D. Marks also acknowledges support on Department of Energy (USA) Grant No. DE-AC02-76ER02995.

Literature Cited

1. Ino, S.; *J. Phys. Soc. Japan* 1966, 21, 346.
2. Ino, S.; Ogawa, T.; *J. Phys. Soc. Japan* 1967, 22, 1369.
3. Heinemann, K.; Poppa, H.; *Appl. Phys. Letts.* 1972, 20, 122.
4. Freeman, L.A.; Howie, A.; Treacy, M.M.J.; *J. Microsc.* 1977, 111, 165.
5. Yacamán, M.J.; Ocana, T.; *Phys. Stat. Sol. (a)* 1977, 42, 571.
6. Treacy, M.M.J.; Howie, A.; Wilson, C.J.; *Phil. Mag. A* 1978, 38, 569.
7. Pennycook, S.J.; *J. Microsc.* 1981, 124, 15.
8. Pennycook, S.J.; Howie, A.; Shannon, M.D.; Whyman, R.; *J. Molecular Catalysis* 1983, 20, 345.
9. Howie, A.; Marks, L.D.; Pennycook, S.J.; *Ultramicroscopy* 1982, 8, 163.
10. Lyman, C.E. In "Catalytic Materials, Relationship Between Structure and Reactivity", American Chemical Society, Washington D.C., 1983, p. 311.
11. Treacy, M.M.J. *ibid.*, p. 367.
12. Baird, T. In "Catalysis"; The Royal Society of Chemistry: London, 1982; Vol 5, p. 172.
13. Marks, L.D.; Smith, D.J.; *J. Crystal Growth* 1981, 54, 425.
14. Smith, D.J.; Marks, L.D.; *J. Crystal Growth* 1981, 54, 433.
15. Marks, L.D.; Smith, D.J.; *J. Microscopy* 1983, 130, 249.
16. White, D.; Baird, T.; Fryer, J.R.; Freeman, L.A.; Smith D.J.; Day, M.; *J. Catal.* 1983, 81, 119.
17. Smith, D.J.; White, D.; Baird, T.; Fryer, J.R.; *J. Catal.* 1983, 81, 107.
18. Sanders, J.V.; *Chemica Scripta* 1978/79, 14, 141.
19. Smith, D.J.; Camps, R.A.; Freeman, L.A.; Hill, R.; Nixon, W.C.; Smith, K.C.A.; *J. Microscopy* 1983, 130, 127.
20. Smith, D.J.; Camps, R.A.; Cosslett, V.E.; Freeman, L.A.; Saxton, W.O.; Nixon, W.C.; Ahmed, H.; Catto, C.J.D.; Cleaver, J.R.A.; Smith, K.C.A.; Timbs, A.E.; *Ultramicroscopy* 1982, 9, 203.
21. Marks, L.D.; Smith, D.J.; *Nature* 1983, 303, 316.
22. Marks, L.D.; *Phys. Rev. Letts.* 1983, 51, 1000.
23. Marks, L.D.; Heine, V.; Smith, D.J.; *Phys. Rev. Letts.* 1983, 52, 656.
24. Smith, D.J.; Marks, L.D.; *Proc. 7th Int. Conf. High Voltage Electron Microscopy*, 1983, p. 53.
25. Marks, L.D.; *Surf. Sci.* 1984, 139, 281.
26. Marks, L.D.; Smith, D.J.; *Surf. Sci.* 1984, 143, 587.
27. Smith, D.J.; Marks, L.D.; submitted to *Ultramicroscopy*.
28. Noonan, J.R.; Davis, H.L.; *J. Vac. Sci. Tech.* 1979, 16, 587.
29. Marks, L.D.; *Ultramicroscopy* 1983/84, 12, 237.
30. Marks, L.D.; Submitted to *Acta Cryst.*
31. Berry, M.V.; *J. Phys. C* 1971, 4, 697.
32. Cowley, J.M.; "Diffraction Physics", 2nd edition, North-Holland: Amsterdam, 1981.
33. Robinson, I.K.; Kuk, Y.; Feldman, L.C.; *Phys Rev. B* 1984, 29, 4762.
34. R.J. Culbertson, private communication.
35. Heine, V.; Marks, L.D.; in preparation

36. van der Merwe, J.H.; Ball, C.A.B. In "Epitaxial Growth"; Matthews, J.W., Ed.; Academic Press: New York, 1975; Part B, p. 493 (see also other articles in both Parts A and B).
37. Neidermeyer, R.; Thin Films 1968, 1, 25.
38. Snyman, J.A.; van der Merwe, J.H.; Surf. Sci. 1974, 42, 190.
39. Wynblatt, P.; in Interatomic Potentials and Simulation of Lattice Defects, (Ed Gehlen, Beeler and Jaffee, Plenum Press, New York, 1972) pp. 633.
40. Snyman, J.A.; Snyman, H.C.; Surf. Sci. 1981, 105, 357.
41. van Hardeveld, R.; Montfoort, V.; Surf. Sci. 1966, 4, 396.
42. Burton, J.J.; Catal. Rev. Sci. Eng. 1974, 9, 209.
43. Andersson, J.R. "Structure of Metallic Catalysts": Academic Press: London, 1975.
44. Marks, L.D.; J. Crystal Growth 1983, 61, 556.
45. Marks, L.D.; Phil Mag A 1984, 49, 81.
46. Howie, A.; Marks, L.D.; Phil Mag. A 1984, 49, 95.
47. Marks, L.D.; Submitted to Surf. Sci.
48. Linford, R.G.; In "Solid State Surface Science"; Green, M., Ed; Marcel Dekker: New York, 1973; Vol. 2, p.1.
49. Flytzani-Stephanopoulos, M.; Schmidt L.D.; Prog. Surf. Sci. 1979, 9, 83.
50. Drechler, M.; In "Surface Mobilities on Solid Materials", Binh, V.T., Ed; Plenum Press: New York and London, 1983; p. 405.
51. Chabai, Y.J.; Rowe, J.E.; Christman, S.B.; Phys. Rev. B. 1981, 24, 3303.
52. Krueger, S.; Monch, W.; Surf. Sci 1980, 99, 157.
53. Lacmann, R.; Springer Tracts in Modern Physics 1968, 44, 1.
54. Metois, J.J.; Spiller, G.D.T.; Venables, J.A.; Phil Mag A 1982, 46, 1015.
55. Buttet, J.; Borel, J.P.; Helv. Phys. Acta, 1983, 56, 541.
56. Yagi, K.; Takayanagi, K.; Kobayashi, K.; Honjo, G.; J. Crystal Growth, 1975, 28, 117.
57. Avery, N.R.; Sanders, J.V.; J Catal. 1970, 18, 129.

RECEIVED March 20, 1985